Uplink Low-Power Scheduling for Delay-Bounded Industrial Wireless Networks Based on Imperfect Power-Domain NOMA

Chaonong Xu, Mianze Wu, Yongjun Xu, and Yuguang Fang, *Fellow, IEEE*

***Abstract*—The power-domain non-orthogonal multiple access (NOMA) supports multiple packet reception, which can be leveraged for delay-bounded applications in industrial wireless networks (IWNs). However, it suffers from high power consumption on transmitters, which poses challenges for battery-powered wireless sensors. Given the delay bound for NOMA-based IWNs, the problem of minimizing aggregate power consumption of transmitters is therefore of great value. In a previous paper, we have addressed the problem under the model of perfect k-successive interference cancellation (k-SIC). In this paper, we study the same problem, however, under the model of imperfect k-SIC, which is more general in theory and more realistic in practice. For the existence of the optimal solution, we first present an explicit sufficient and necessary condition, which correlates three key parameters of network system together. We also propose a polynomial-time optimal algorithm with complexity $O(n^2)$. We further consider the same problem with discrete transmit powers, and present an approximation algorithm with complexity $O(n^2)$. Performance evaluation reveals that the delay bound requirement has tremendous impacts on both the aggregate power consumption and the maximum transmit power. Relative to the perfect SIC, the residual error caused by imperfect SIC results in extra power consumption of transmitters. However, the extra power consumption is gradually diminished with the further relaxation of the delay bound.**

***Index Terms*—Delay guarantee, low power, power control, successive interference cancellation (SIC), uplink scheduling.**

I. Introduction

In INDUSTRIAL wireless networks (IWNs), wireless sensors are usually deployed to sense the status of industrial processes and then, feedback the results to a sink. As a special case of wireless sensor networks, IWNs are usually cellular-style instead of *ad hoc*, because of the rigid requirements in industrial applications. Therefore, physical and MAC layer protocols with low latency, high reliability, and low power are research focuses in IWNs. Distinct from both the delay-tolerant wireless sensor networks and the delay-sensitive ultra-reliable low-latency communications (URLLC), some industrial applications, such as [2] and [3], are delay bounded. In other words, the UL (uplink) transmissions should be delay guaranteed for these applications in IWNs. Therefore, the guaranteed medium access delay is of vital importance to IWNs.[1]

Although the traditional time division multiple access (TDMA) has the advantage of providing delay guarantee, its medium access delay which equals the polling time would be high if there are massive wireless sensors. Relatively, since non-orthogonal multiple access (NOMA) can shorten the polling time drastically by supporting multiple parallel transmissions, it is suitable for delay-bounded applications in IWNs [4]. The power-domain NOMA, which is based on successive interference cancellation (SIC) receivers, is now under full consideration for industrial applications or heterogeneous cellular networks because of its support for massive connections [5]. However, tremendous electric energy on wireless sensors will be consumed for overcoming high interferences, which is an inherent shortcoming of the power-domain NOMA.[2] Obviously, the shortcoming poses great challenges for the battery-powered wireless sensors. Thus, the problem of minimizing the aggregate power consumption of wireless sensors[3] with delay guarantee for NOMA-based IWNs is of practical value.

To solve the problem, joint optimization of power controlling and UE scheduling is utilized. On one hand, the UE scheduling determines which UEs will transmit in parallel, i.e., how to group UEs. On the other hand, suitable transmit powers are set by power controlling so that signals of all parallel UEs can be decoded successfully by an SIC receiver.

Under the assumption of perfect SIC, i.e., there is no residual error for SIC, we design an efficient low-power scheduling scheme with complexity $O(n^2)$ in [1]. However, as we know, the perfect SIC is impossible in practice, and therefore, we need to

Manuscript received January 30, 2019; revised June 2, 2019 and June 17, 2019; accepted June 18, 2019. This work was supported by the National Natural Science Foundation of China under Grant 61702487. *(Corresponding author: Chaonong Xu.)*

C. Xu and M. Wu are with the Beijing Key Lab of Petroleum Data Mining, China University of Petroleum, Beijing 102249, China (e-mail: xuchaonong@cup.edu.cn).

Y. Xu is with the Institute of Computing Technology, China Academy of Sciences, Beijing 100190, China (e-mail: xyj@ict.ac.cn).

Y. Fang is with the Department of Electrical and Computer Engineering, University of Florida, Gainesville, FL 32611 USA (e-mail: fang@ece.ufl.edu).

Digital Object Identifier 10.1109/JSYST.2019.2924483

[1]Generally speaking, the uplink transmission delay in IWNs consists of queuing delay and medium access delay. However, since the queuing delay is influenced by so many factors, and is hard to be precisely modeled and tracked, we only consider the medium access delay in this paper.

[2]In general, in power-domain NOMA, the power consumptions of transmitters increase exponentially with the enhancement of its parallel receiving capability. It can also be verified from Sections VII-A and VII-B.

[3]For convenience, in this paper, wireless sensor is abbreviated as UE (user equipment).

find valid algorithms for the same problem under the imperfect SIC.

Under imperfect SIC, since the residual errors left by canceling previous signals bring interferences to successive signals, the low-power scheduling problem is more complex than that under perfect SIC. Therefore, although the optimal solution to low-power scheduling is presented under perfect SIC model [1], we doubt the existence of the optimal solution under imperfect SIC. So, we conduct further studies in this paper, prove the existence of the optimal solution, and present some low-complexity algorithms for finding the optimal solution.

Our technical contributions are as follows.

1) We present an explicit sufficient and necessary condition for the existence of a feasible power solution for imperfect SIC. To the best of our knowledge, this paper presents the first feasibility result in the field of imperfect SIC.

2) We formulate the low-power scheduling problem as a mixed integer optimization problem by the joint UE scheduling and power allocation. By defining a key term named r-PTSI (power threshold sequence for imperfect r-SIC), we first reveal the structural characteristic of the optimal solution and then, propose a low-complexity optimal algorithm based on the structural characteristic.

3) We also propose an approximation algorithm with complexity $O(n^2)$ for the same problem with discrete transmit power levels, which must be dealt with for practicability,[4] and an approximation ratio is also presented.

Since both the model and the theoretic basis are distinct from those in [1], we declare that this paper is absolutely not a simple modification of [1], but a generalized extension to the imperfect SIC instead.

The remainder of this paper is organized as follows. Section II reviews the related works, and Section III presents the system models. Preliminaries are introduced in Section IV. Problem formulation and solution are introduced and analyzed in Section V. Based on the conclusions drawn in Section V, the same problem with discrete transmit powers is considered in Section VI. Performance evaluations are presented in Section VII, and conclusions are drawn in Section VIII.

II. Related Works

Nowadays, power-domain NOMA technologies receive extensive research efforts from wireless communications and networking fields [6]–[8]. The performance of power-domain NOMA is directly influenced by the capability of SIC receivers. Most early works focus on downlinks; we refer readers to [9] for an overview. As to the MAC protocols of the SIC-based network system, they can be categorized as random access-based and scheduling-based. For the random access-based algorithms, now there are three typical solutions, which are based on low-density parity-check codes [10], compressive sensing [11], and game theory [12], respectively. However, we only focus on the two related fields, i.e., scheduling-based low-power MAC algorithms and the imperfect SIC, in this paper.

1) Studies on the energy consumption in UL: Energy efficiency is an important aspect of power-domain NOMA [13]. Zhang *et al.* [14] reveal that to save UEs' power consumption, the transmit powers should be allocated based on the channel gains of UEs. In [6], fixed power allocation is introduced for two UEs such that the achieved UEs' rates are improved relative to the conventional orthogonal multiple access. We also minimize the aggregate power of UEs in [1] under the perfect k-SIC model, and present a tractable and optimal algorithm by means of a two-stage decomposition.

2) Studies of imperfect SIC: The imperfect SIC is now attaining more and more interests, where the linear residual error model, which is first discussed in 2003 [15], is being widely adopted [16]. Tweed *et al.* [17] optimize the aggregate power consumption of transmitters in the multichannel scenario, and an iterative convex optimization algorithm is utilized to solve the problem. Also, using the linear residual error model, Celik *et al.* [18] optimize the downlink capacity based on clustering and power-bandwidth tradeoff by formulating it as a mix-integer nonlinear programming problem. In [16], the fairness of transmit powers in UL MIMO-NOMA networks with imperfect SIC is formulated as a universal nonconvex optimization problem and solved by an approximation algorithm. We, however, present a closed-form solution to the aggregate power minimization problem on imperfect SIC, and propose a tractable optimal algorithm for the problem, instead of the time-consuming optimization-based algorithms.

III. System Model

We consider a single-hop, single-channel wireless network consisting of n single-antenna UEs[5] $u_1, u_2, \ldots, u_n$, and a single-antenna sink. The sink is equipped with a k-SIC receiver. A k-SIC receiver can decode at most k signals at one time, provided that SINR (signal-to-interference-plus-noise ratio) of every signal after interference cancellation is higher than the decoding threshold of the receiver. We assume that all of the n UEs have data to transmit.[6] Note that we focus on the uplinks, therefore, SIC receivers are not required for the UEs which are the transmitters. Fig. 1 plots a network example comprised of three UEs and a 2-SIC based sink.

The residual error of SIC is mainly caused by factors such as imperfect amplitude and phase estimation. Since they are closely related to the preamble power, the residual error is thought to be linear with the signal receive power, i.e., if the signal power

[4]The transmit power is not continuously adjustable for any transceiver nowadays. Take CC1000 which is manufactured by TI for example, there are 30 feasible power levels from −20 to 10 dBm with a constant step size 1 dBm. Therefore, if the transmit power calculated lies between two neighbor steps, in fact, it is infeasible for commercial-off-the-shelf radio transceiver.

[5]In this paper, UE, user, and transmitter are used interchangeably, and receiver is equivalent to sink.

[6]At the beginning of a frame, those UEs which have transmission tasks will report themselves to the sink via the control channel. Since we only need to find the UEs which try to be transmitters of the upcoming frame, methods such as [19], which is based on compressive sensing, can achieve the goal with low overhead.

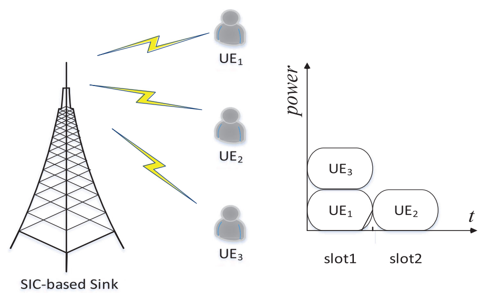

Fig. 1. Uplink transmissions with an SIC-based sink.

TABLE I
NOTATIONS

S	user scheduling strategy
$S[i]$	users in the ith slot of scheduling strategy S
G_i	channel gain of u_i
L	frame length bound
$(\widehat{X}_r^{(r)}, \cdots, \widehat{X}_1^{(r)})$	power threshold sequence for r-SIC
p_i	transmit power of u_i
$tp_i^{(\rho\gamma)}$	continuous transmit power of u_i in the optimal solution when the decoding threshold is $\rho\gamma$
$tp_i^{(\gamma)}$	continuous transmit power of u_i in the optimal solution when the decoding threshold is γ
$\widehat{tp}_i^{(\gamma)}$	discrete transmit power of u_i in the optimal solution when the decoding threshold is γ
$\{\overline{tp}_m, \cdots, \overline{tp}_1\}$	feasible discrete transmit powers set
$[\![x]\!]$	$\underset{y \in \overline{TP} \bigcap (y \geq x)}{\arg\min} \quad (y-x), (x \geq 0)$
$T_b, \quad T_s$	transmission delay bound, sampling cycle

of a UE at a receiver is p, its residual error after interference cancellation is εp, where ε is the residual coefficient. As we have stated in Section II, recently, the residual model has been widely adopted.

We use a parameter G_i to capture the loss of signal power, as the signal propagates through the wireless channel from u_i to the sink. Therefore, the received power at the sink is $G_i p_i$, if the transmit power of u_i is p_i. Besides, we also assume that channel gains of all UEs remain constant during a frame, which is realistic for slow fading channels. For convenience, the parameters used in this paper are listed in Table I.

Similar to [1], in the considered network, time is divided into frames, and each frame includes multiple time slots. We assume that the time span of a slot is enough to deliver a data packet. In fact, the above-mentioned assumptions are in accordance with practical applications in IWNs [2].

For k-SIC, there are at most k UEs which transmit simultaneously, and they will be decoded successively by SIC decoder. The term phase is defined to depict the decoding order, where the UE decoded first is said to occupy the decoding phase 1, the second UE is for phase 2, and so on.

IV. Preliminaries

A. Ordering Inequality Theorem

The ordering inequality is a well-known theorem as follows. Assume $a_1 \geq a_2 \geq \cdots \geq a_n, b_1 \leq b_2 \leq \cdots \leq b_n$. The optimal solution to the problem

$$\min_{X_{ij}} \sum_{i,j=1,\ldots,n} X_{ij} a_i b_j$$

$$\text{s.t.} \quad X_{ij} \in \{0,1\}$$
$$\sum_{i=1,\ldots,n} X_{ij} = 1 \text{ for all } j \in [1,n]$$
$$\sum_{j=1,\ldots,n} X_{ij} = 1 \text{ for all } i \in [1,n]$$

is $X_{ij} = \begin{cases} 1 & \text{for all } i = j \\ 0 & \text{for all } i \neq j. \end{cases}$

We also present a proof for the theorem in [1].

B. Minimum Power Allocation for r Parallel Transmitters

Definition 1: Minimum power allocation for r parallel transmitters (MPAr PT): Given is an uplink toy network consisting of an imperfect k-SIC receiver and r transmitters $u_1, u_2, \ldots, u_r$ with channel gains as $G_1, G_2, \ldots, G_r$, respectively. Without loss of generality (WLOG), we assume that $G_1 \leq G_2 \leq \cdots \leq G_r, r \leq k$, and n_0 is the noise power. Denote transmit powers of $u_1, u_2, \ldots, u_r$ by $p_1, p_2, \ldots, p_r$, respectively. Assign value for $p_1, p_2, \ldots, p_r$ so that the aggregate power consumption of the r transmitters is minimized under the premise that $u_1, u_2, \ldots, u_r$ transmit simultaneously and their signals are all decoded successfully.

This problem is thus formulated as

$$\min_{\{p_1,p_2,\ldots,p_r\}} \sum_{i=1}^{r} p_i$$

$$\text{s.t.} \quad \frac{G_i p_i}{I_i + n_0} \geq \gamma; \quad p_i \geq 0 \qquad \forall i \in [1,r].$$

To solve MPAr PT, we have to first know I_i, i.e., the interference to u_i. Obviously, I_i is decided by the decoding order and the model of residual error, provided that $\{p_1, p_2, \ldots, p_r\}$ are known. Lemma 1 reveals that to achieve the optimal solution to MPAr PT, the transmitters' signals must be decoded in the descending order of channel gains.

Lemma 1: If $\gamma > 1$, the optimal decoding order for MPAr PT is the descending order of the channel gain of transmitters.[7,8]

Proof. Please refer to the proof of Lemma 1 in [1]. ■

Based on Lemma 1 and the model of residual error, MPAr PT can, therefore, be reformulated as follows:

$$\min_{\{p_1,\ldots,p_r\}} \sum_{i=1}^{r} p_i \tag{1a}$$

[7]Since any signal could be decoded only if its power is greater than its interference power, $\gamma > 1$ is not a stringent constraint in practice.

[8]The optimal decoding order is distinct from that in [6] because the optimization object is the throughput instead of the power consumption there.

$$\text{s.t.}\quad \frac{G_r p_r}{\sum_{i=1}^{r-1} G_i p_i + n_0} \ge \gamma \tag{1b}$$

$$\frac{G_l p_l}{\sum_{i=1}^{l-1} G_i p_i + \varepsilon \sum_{i=l+1}^{r} G_i p_i + n_0} \ge \gamma \quad \forall l \in [2, r-1] \tag{1c}$$

$$\frac{G_1 p_1}{\varepsilon \sum_{i=2}^{r} G_i p_i + n_0} \ge \gamma. \tag{1d}$$

Before we start to solve the MPAr PT problem, the following key definition is given.

Definition 2: Power threshold sequence for imperfect r-SIC (r-PTSI) is a sequence $\widehat{X}^{(r)} = (\widehat{X}_r^{(r)}, \widehat{X}_{r-1}^{(r)}, \ldots, \widehat{X}_1^{(r)})^T$ which satisfies the following group of equalities:

$$\begin{cases} \frac{\widehat{X}_r^{(r)}}{\sum_{i=1}^{r-1} \widehat{X}_i^{(r)} + n_0} = \gamma & (2a) \\ \frac{\widehat{X}_l^{(r)}}{\sum_{i=1}^{l-1} \widehat{X}_i^{(r)} + \varepsilon \sum_{i=l+1}^{r} \widehat{X}_i^{(r)} + n_0} = \gamma \quad \forall l \in [2, r-1] & (2b) \\ \frac{\widehat{X}_1^{(r)}}{\varepsilon \sum_{i=2}^{r} \widehat{X}_i^{(r)} + n_0} = \gamma & (2c) \end{cases}$$

where $\widehat{X}_i^{(r)} > 0$ for all $i \in [1, r]$ and $\gamma > 1$.

Obviously, $\widehat{X}_r^{(r)} \ge \widehat{X}_{r-1}^{(r)} \ge \cdots \ge \widehat{X}_1^{(r)}$, and all of them are related to ε. Next, we present a key property of r-PTSI, which will be used in Lemma 3.

Lemma 2: For $r \ge 2$, r-PTSI exists if and only if $\varepsilon\delta^r < 1$ where $\delta = \frac{(\gamma+1)}{(1+\gamma\varepsilon)}$. Besides, r-PTSI is of a geometric series.

Proof. Please refer to Appendix A. ■

Next, in Lemma 3, we show that, if all "=" in (2a)–(2c) are replaced with "≥," r-PTSI is the minimum feasible solution to the inequality group.

Lemma 3: Let

$$A = \begin{pmatrix} 1 & -\gamma & -\gamma & \cdots & -\gamma & -\gamma \\ -\varepsilon\gamma & 1 & -\gamma & \cdots & -\gamma & -\gamma \\ -\varepsilon\gamma & -\varepsilon\gamma & 1 & \cdots & -\gamma & -\gamma \\ \cdots & \cdots & \cdots & \cdots & \cdots & \cdots \\ -\varepsilon\gamma & -\varepsilon\gamma & -\varepsilon\gamma & -\varepsilon\gamma & \cdots & 1 \end{pmatrix}_{r\times r}$$

and $X = (X_r, X_{r-1}, \ldots, X_1)^T$, $N = n_0\,(\gamma, \gamma, \ldots, \gamma)^T$. We have the following conclusions.

1) There is a non-negative elementary row transformation matrix $T_{r\times r}$, such that

$$B = TA = \begin{pmatrix} 1 & -\gamma & -\gamma & \cdots & -\gamma & -\gamma \\ 0 & a_1 & b_{23} & b_{24} & \cdots & b_{2r} \\ 0 & 0 & a_2 & b_{34} & \cdots & b_{3r} \\ \cdots & \cdots & \cdots & \cdots & \cdots & \cdots \\ 0 & 0 & 0 & 0 & \cdots & a_{r-1} \end{pmatrix}_{r\times r}.$$

Besides, $b_{ij} \le 0$ for all $i < j$, where $i \in [2, r-1]$ and $j \in [3, r]$.

2) If and only if $\varepsilon\delta^r < 1$, where $\delta = \frac{\gamma+1}{\varepsilon\gamma+1}$, $a_i > 0$ holds for all $i \in [1, r-1]$.

3) If $a_i > 0$ for all $i \in [1, r-1]$, for any positive vector $\overline{X}$ satisfying $A\overline{X} \ge N$, $\overline{X} \ge \widehat{X}^{(r)}$ holds where $\widehat{X}^{(r)}$ is r-PTSI.

4) If $\exists i \in [1, r-1]$ such that $a_i \le 0$, the inequality group $AX \ge N$ has no positive real solutions.

Proof. Please refer to Appendix B. ■

Based on the conclusions of Lemma 3, Theorem 1 tells the optimal solution to the MPAr PT problem.

Theorem 1: 1) If and only if $\varepsilon\delta^r < 1$, the optimal solution to MPAr PT is $\left(\frac{\widehat{X}_r^{(r)}}{G_r}, \frac{\widehat{X}_{r-1}^{(r)}}{G_{r-1}}, \ldots, \frac{\widehat{X}_1^{(r)}}{G_1}\right)$, where $\left(\widehat{X}_r^{(r)}, \widehat{X}_{r-1}^{(r)}, \ldots, \widehat{X}_1^{(r)}\right)^T$ is r-PTSI.

2) If $\varepsilon\delta^r \ge 1$, the MPA$r$ PT problem has no feasible solutions.

Proof. Please refer to Appendix C. ■

We have further explanation for Theorem 1 as follows.

1) $\varepsilon\delta^r < 1$ is a sufficient and necessary condition for the existence of the optimal solution to MPAr PT, and besides, the optimal solution is $\left(\frac{\widehat{X}_r^{(r)}}{G_r}, \frac{\widehat{X}_{r-1}^{(r)}}{G_{r-1}}, \ldots, \frac{\widehat{X}_1^{(r)}}{G_1}\right)$.

2) According to the well-known conclusion in the power control literature [20],[9] a sufficient and necessary condition for feasible powers is that $\rho(I - A) < 1$, where $\rho(I - A)$ is the spectral radius of the matrix $I - A$, and I is identity matrix. However, although the conclusion is useful, we have difficulties in acquiring an explicit expression for the spectral radius of $I - A$. Lemma 3 utilizes the structural particularity of A, and presents an explicit and concise condition, i.e., $\varepsilon\delta^r < 1$, for the existence of feasible solutions.[10]

V. Minimum Low-Power Scheduling Algorithm for Imperfect k-SIC

Definition 3: Real-time minimum low-power scheduling for imperfect k-SIC (RMLPSI-k SIC) problem: given an imperfect k-SIC receiver and n transmitters $u_1, u_2, \ldots, u_n$ with channel gains $G_1, G_2, \ldots, G_n$, respectively, WLOG, we assume $G_1 \le G_2 \le \cdots \le G_n$. Noise power is n_0 for all transmitters. Denote their transmit powers by $p_1, p_2, \ldots, p_n$, respectively, and assume that each of them is a continuous variable,[11] such that the aggregate power consumption of the n transmitters is minimized under the following constraints: 1) every transmitter is scheduled only once in a frame;[12] 2) the frame length is no greater than the given value L; and 3) SINR for every UE is above the given decoding threshold γ.

[9] Although the mathematical formulation of our problem is similar to that in [20], they are distinct in the application essence: [20] is for finding a feasible solution to the problem of UE–UE communications on regular radio, while our paper is for UEs-BS communication on imperfect SIC radio.

[10] In reality, r is a small integer because the implementation complexity of k-SIC must be constrained, and ε is a very small decimal for accurate interference cancellation techniques, and therefore, the condition is easy to be satisfied. We provide some numerical examples for it in Section VII-C of this paper.

[11] In fact, there is no absolute continuous power variable in practice. However, if the power levels are numerous enough and the power spacing is small enough, the output powers can be considered to be continuous.

[12] The constraint is set intentionally for fairness if the wireless sensors have similar throughput requirements.

Thus, the RMLPSI-k SIC problem can be formulated as a mixed integer optimization problem

$$\min_{\{t_1,t_2,\ldots,t_n\},\{p_1,p_2,\ldots,p_n\}} \sum_{i=1}^{n} p_i \tag{3a}$$

$$\text{s.t.} \quad 0 \le \sum_{i=1}^{n} 1(t_i = j) \le k \qquad \forall j \in [1, L] \tag{3b}$$

$$t_i \in [1, \ldots, L] \qquad \forall i \in [1, n] \tag{3c}$$

$$\frac{G_i p_i}{I_i + n_0} \ge \gamma; \quad p_i \ge 0 \quad \forall i \in [1, n] \tag{3d}$$

where t_i represents the scheduling slot index for u_i, $1(.)$ is the indicator function, and I_i is the power of interference when decoding signal from u_i. Apparently, the interference is only influenced by $\{t_1, t_2, \ldots, t_n\}$ if $\{p_1, p_2, \ldots, p_n\}$ are known. L is the frame length bound, which is for gauging the real-time performance.[13,14]

RMLPSI-k SIC is a joint optimization of power controlling and UE scheduling. Next, based on Theorem 1, we show that RMLPSI-k SIC can be solved by a low-complexity algorithm, since power controlling and UE scheduling is decoupled based on Theorem 1, which converts the joint optimization problem into a two-stage optimization problem.[15]

Using Theorem 1 in Section IV, we now start to solve the RMLPSI-k SIC problem. Lemma 4 reveals a key structural characteristic of the optimal solution to the RMLPSI-k SIC problem, i.e., the number of slots and the decoding phases in each slot of the optimal solution.

Lemma 4: If $n \le kL$, for the optimal solution to RMLPSI-k SIC, we have the following.

1) The number of UEs scheduled in any slot is either $\lfloor n/L \rfloor$ or $\lceil n/L \rceil$.

2) There are $L\lceil n/L \rceil - n$ slots, each of which has $\lfloor n/L \rfloor$ UEs, and $L - L\lceil n/L \rceil + n$ slots, each of which has $\lceil n/L \rceil$ UEs.

Proof: Please refer to Appendix D. Its proof is similar to that of Lemma 2 in [1], with a small hint that $\widehat{X}_i^{(r)} < \widehat{X}_{i+1}^{(r)}$ for any $i \in [1, r-1]$.

Lemma 4 reveals that to achieve low power consumption, UEs should be equally allocated to all slots as far as possible. In other words, it has no relationship with k if $n \le kL$ holds. Obviously, it completely coincides with intuitions, because uniformly grouped UEs is beneficial for lowering aggregate power consumptions. Based on the lemma, instead of searching the entire strategy space for finding the optimal UEs scheduling strategy, we only need to compare the aggregate power consumption of these scheduling strategies consistent with Lemma 4, instead of searching the entire strategy space. Algorithm 1 is designed based on the above-mentioned guidelines.

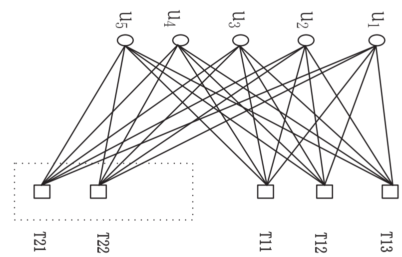

Fig. 2. Example of $GH(5, 3, 2)$.

Algorithm 1: Optimal Algorithm for RMLPSI-k SIC{.

// Input: n, k, L, which satisfies $kL \ge n$.
// Output: optimal scheduling strategy for the n users.
1. $GH(n, k, L) = \phi$; compute $\lceil n/L \rceil$-PTSI as $\widehat{X}^{(\lceil n/L \rceil)}$, $\lfloor n/L \rfloor$-PTSI as $\widehat{X}^{(\lfloor n/L \rfloor)}$; $M = \widehat{X}^{(\lceil n/L \rceil)}_{\lceil n/L \rceil}/G_1$;
2. add n graph nodes with label u_i where $i \in [1, n]$ into part I of $GH(n, k, L)$;
3. add $L\lfloor n/L \rfloor$ graph nodes with label T_{hj} where $h \in [1, L]$ and $j \in [1, \lfloor n/L \rfloor]$ into part II of $GH(n, k, L)$;
4. if $(n\%L!=0)${
5. for(i=1; $i \le n\%L$; i++) add a graph node with label $T_{i\lceil n/L \rceil}$ into part II of $GH(n, k, L)$; }
6. for any graph node u_i in part I{
7. for any graph node T_{hj} in part II {
8. if $(h \le L - L\lceil n/L \rceil + n)$ add edge (u_i, T_{hj}) with weight $-\widehat{X}_j^{(\lceil n/L \rceil)}/G_i + M$;
9. else add edge (u_i, T_{hj}) with weight $-\widehat{X}_j^{(\lfloor n/L \rfloor)}/G_i + M$; }}
10. find a maximum weight matching (MWM) of the complete bipartite graph;
11. for any (u_i, T_{hj}) in the MWM, if $h \le L - L\lceil n/L \rceil + n$, u_i will be scheduled in the hth slot with power $\widehat{X}_j^{(\lceil n/L \rceil)}/G_i$, else u_i will be scheduled in the hth slot with power $\widehat{X}_j^{(\lfloor n/L \rfloor)}/G_i$;}

Lines 2–9 in Algorithm 1 generate a balanced complete bipartite graph $GH(n, k, L)$. The nodes in part I of the bipartite graph correspond to all UEs. From lines 3–5, all possible decoding positions are acted as part II of the bipartite graph. The edge (u_i, T_{hj}) means that u_i could be scheduled in the slot h, and decoded at phase j of the slot h. Lines 7–9 are for setting the weight of graph edge. Based on Theorem 1, the weight of the edge (u_i, T_{hj}) is directly related with the minimal transmit power for u_i to be decoded at the phase j of slot h. Fig. 2 is an example of $GH(5, 3, 2)$ where edge weights are omitted for clarity. M is set deliberately just for keeping the weight of every edge a positive number. Thus, the MWM of $GH(n, k, L)$

[13] To achieve the guaranteed real-time performance, the time span of a frame must be no longer than half of the transmission delay bound in typical settings. Their relationship will be revealed in detail in Section VII-C.

[14] The constraint of the maximal transmit power is not considered because it hinders us from presenting an analytical expression of the optimal powers. Since we aim to minimize the aggregate power consumption, the optimal transmit powers of UEs must not be very large, i.e., the constraint of maximal power is not a tight constraint in general, and thus, can be removed without any impacts. This assertion is also verified in the section of performance evaluations.

[15] Although the overall idea of this section is similar with the Section IV-B in [1], there is a lot of fine-grained distinctness in almost all proofs and algorithms. It is the imperfection of SIC which causes all of the distinctness.

corresponds to a feasible scheduling strategy. Now, Theorem 2 shows that the scheme mapped from the MWM is optimal.

Theorem 2: If and only if $\varepsilon\delta^{\lceil n/L \rceil} < 1$, Algorithm 1 outputs an optimal solution to RMLPSI-k SIC.

Proof. Please refer to Appendix E. ■

In Algorithm 1, we determine the optimal UE grouping strategy in line 10, and then, allocate optimal transmit powers for every slot in line 11. In other words, UE scheduling and power allocation in RMLPSI-k SIC could be decoupled,[16] and therefore, the computation complexity is greatly reduced. It is k-PTSI that separates power allocation and UE scheduling in the RMLPSI-k SIC problem without impairing the optimality. Thus, k-PTSI is key to the correctness of the optimal algorithm.

If the MWM in the tenth line of Algorithm 1 is found by Kuhn–Munkres algorithm [21], the time complexity of Algorithm 1 is $O(n^3)$ since that of Kuhn–Munkres algorithm is $O(n^3)$, and the complexity for setting up the graph is $O(n^2)$. Next, we present a faster algorithm for finding an MWM of the graph because it is a balanced complete bipartite graph.

Algorithm 2 is more complex than [1, Algorithm 2], where the perfect SIC is assumed. The intrinsic reason for the distinction of the two algorithms is that for any $i \in [1, r-1]$, $\widehat{X}_i^{(r)} = \widehat{X}_i^{(r-1)}$ holds for perfect SIC, while $\widehat{X}_i^{(r)} > \widehat{X}_i^{(r-1)}$ holds for imperfect SIC, which brings complexity in allocating slots for UEs.

Lines 1–4 of Algorithm 2 is for initialization, where $Phases$ saves all elements from both $\lfloor n/L \rfloor$-PTSI and $\lceil n/L \rceil$-PTSI. For any element of $Phases$, its $value$ is from $\lfloor n/L \rfloor$-PTSI if its $type$ is NF, otherwise, it is from $\lceil n/L \rceil$-PTSI if its $type$ is FU. In line 5, $Phases$ are reordered and saved to $Stphases$ in ascending order of the $value$ field. From lines 6–13, although it is implicit, we virtually construct n decoding positions T_{ij}, where $i \in [1, L]$ and $j \in \begin{cases} [1, \lfloor n/L \rfloor], & \text{if} \quad i \in [1, L\lceil n/L \rceil - n] \\ [1, \lceil n/L \rceil], & \text{if} \quad i \in [L\lceil n/L \rceil - n + 1, L] \end{cases}$, and the value of T_{ij} is $\begin{cases} \widehat{X}_j^{(\lfloor n/L \rfloor)}, & \text{if} \quad i \in [1, L\lceil n/L \rceil - n] \\ \widehat{X}_j^{(\lceil n/L \rceil)}, & \text{if} \quad i \in [L\lceil n/L \rceil - n + 1, L]. \end{cases}$ Then, the n UEs are mapped to the n decoding positions based on the principle that u_l should be mapped to the lth element in the ascending value of T_{ij}. In fact, the mapping is closely related with the ordering inequality theorem.

Theorem 3: Algorithm 2 outputs an MWM of $GH(n, k, L)$.

Proof. Please refer to Appendix F. The core of the proof is the ordering inequality theorem. ■

Theorem 3 reveals that for the optimal solution, the channel gain of any UE decoded in decoding phase i must be greater than that of any UE decoded in decoding phase $i+1$, where $i \in [1, k-1]$.

The complexity of Algorithm 2 is determined by the sorting algorithm used in line 5 of Algorithm 2. Generally, it is $O(n \log n)$ if the classic quick sorting algorithm is adopted. Therefore, the time complexity of Algorithm 1 is thus $O(n^2)$ if its tenth line is replaced by Algorithm 2.

[16]First, Lemma 4 narrows the searching space. Second, Theorem 1 reveals that for any UE scheduling strategy, its optimal power allocation strategy is analytically known. Therefore, for any given UE scheduling strategy, we can compute its minimal aggregate power consumption. By comparing the minimal aggregate power consumption of these UE scheduling strategies which are in the above narrowed strategy space, we can find the optimal UE scheduling strategy. Obviously, with respect to that of the original blind searching method, its computation complexity will be reduced greatly.

Algorithm 2: Faster Algorithm for MWM of $GH(n, k, L)${.

// Input: $GH(n, k, L), n, k, L$; Output: MWM of $GH(n, k, L)$;
struct phase {bool type; int phid; int value}:
Phases[$\lfloor n/L \rfloor + \lceil n/L \rceil$], Stphases[$\lfloor n/L \rfloor + \lceil n/L \rceil$];
1. $OUT = \phi$;
2. sort $u_1, u_2, \ldots, u_n$ in the ascending order of their channel gains, WLOG, assume $G_1 \leq G_2 \leq \cdots \leq G_n$;
3. for ($j = 1; j \leq \lfloor n/L \rfloor; j++$) {
 $Phases$[j].type=NF; $Phases$[j].phid=j;
 $Phases$[j].value=$\widehat{X}_j^{(\lfloor n/L \rfloor)}$;}
4. for ($j = 1; j \leq \lceil n/L \rceil; j++$) {
 $Phases$[j+$\lfloor n/L \rfloor$].type=FU;
 $Phases$[j+$\lfloor n/L \rfloor$].phid=j;
 $Phases$[j+$\lfloor n/L \rfloor$].value = $\widehat{X}_j^{(\lceil n/L \rceil)}$;}
5. sort $Phases$ based on its $value$ field in the ascending order, and save the ordered results into array $Stphases$;
6. idx=1;
7. for ($j = 1; j \leq \lfloor n/L \rfloor + \lceil n/L \rceil; j++$) {//each $Stphases$
8. if ($Stphases[j]$.type==NF) {//process NF-type phase
9. for (k=1; $k \leq L\lceil n/L \rceil - n$; k++,$idx$++) {
10.   add $(u_{idx}, T_{(k)(Stphases[j].phid)})$ into OUT;}}
11. else { //process FU-type phase
12.   for (k=1; $k \leq L - L\lceil n/L \rceil + n$; k++,$idx$++){
13. add $(u_{idx}, T_{(L\lceil n/L \rceil - n + k)(Stphases[j].phid)})$ into OUT;}}

VI. Minimum Discrete Low-Power Scheduling for Imperfect k-SIC

Assume there are m transmit power levels $\overline{tp}_m, \overline{tp}_{m-1}, \ldots, \overline{tp}_1$ where $\overline{tp}_m > \overline{tp}_{m-1} > \cdots > \overline{tp}_1$, and $\frac{\overline{tp}_{i+1}}{\overline{tp}_i} = \rho$ for $\forall i \in [1, m-1]$. The real-time minimum discrete low-power scheduling for imperfect k-SIC (RMDLPSI-k SIC) problem is formulated as follows:

$$\min_{\{t_1,\ldots,t_n,p_1,\ldots,p_n\}} \sum_{i=1}^{n} p_i \tag{4a}$$

$$s.t. \quad p_i \in \overline{TP} \qquad \forall i \in [1, n] \tag{4b}$$

$$(2b); \qquad (2c); \qquad (2d) \tag{4c}$$

where $\overline{TP} = \{\overline{tp}_m, \overline{tp}_{m-1}, \ldots, \overline{tp}_1\}$ is a feasible power set. Obviously, compared with RMLPSI-k SIC, there is an extra constraint (4b), i.e., the constraint of feasible transmit power.

Define $[x] = \arg\min_{(y \in \overline{TP}) \cap (y \geq x)} (y - x), (x \geq 0)$, in other words, $[x]$ is the value that satisfies: 1) it belongs to the set $\overline{TP}$ and 2) it is no less than x and the nearest to x.

Algorithm 3: Approximation Algorithm for RMDLPSI-k SIC{.

1. use Algorithm 1 to solve RMLPSI-k SIC with decoding threshold being $\rho\gamma$;
2. assume that the transmit power for UE_i is $tp_i^{(\rho\gamma)}$;
3. for every u_i {adjust its transmit power as $[tp_i^{(\rho\gamma)}]$}; }

RMDLPSI-k SIC is a combinatorial optimization problem, which is generally NP-hard. Therefore, based on Algorithm 1, we propose an approximation algorithm for RMDLPSI-k SIC.

Obviously, Algorithm 3 is valid only if $\varepsilon\delta_{(\rho\gamma)}{}^{\lceil n/L \rceil} < 1$, where $\delta_{(\rho\gamma)} = \frac{\rho\gamma+1}{1+\rho\gamma\varepsilon}$, since the solution output by Algorithm 1 is valid under that condition.

Theorem 4: 1) Algorithm 3 outputs a feasible solution to the RMDLPSI-k SIC problem.

2) The approximation ratio of Algorithm 3 is no larger than $\rho^{(\lceil n/L \rceil+1)}$.

Proof. Please refer to Appendix G. ■

Obviously, the complexity of Algorithm 3 is still $O(n^2)$.

VII. Performance Evaluations

We conduct some simulation experiments to evaluate the effectiveness of the algorithms presented in this paper. Some simulation parameters are set as follows. To reveal the effect of the residual error on the performance of aggregate power consumption, the residual coefficient varies from 0 to 0.1. The noise power spectral density is -169 dBm/Hz and the channel bandwidth is 200 kHz, thus, n_0 is -116 dBm. The signal frequency is 2.4 GHz and the decoding threshold γ is two. The regular transceiver that does not support SIC is represented by $k = 1$. The minimum discrete transmit power $\overline{tp}_1$ is -25 dBm and ρ is 3 dB. The channel gain model for WLAN signal is $CG = -20\log(f) - 26\log(d) + 19.2$, where f is the frequency in megahertz, and d is the Euclidean distance between the transmitter and receiver in meters. Using the channel gain model, the channel gain of each UE can be known based on its Euclidean distance with the sink.

A wireless network consisting of 30 UEs and one sink is considered. The sink is at the center of a square with side length of 120 m, and UEs are placed uniformly in the square.

A. Power Consumption With Limited Frame Length

The relationship between the aggregate power consumption and the frame length bound is revealed in this experiment. In practical applications, the requirements of the specific applications, i.e., the UE number and the real-time requirement, are known in general. Therefore, a k-SIC receiver should be selected where $k = \lceil \frac{n}{L} \rceil$. Of course, all of the n UEs must be in the receiving area of the receiver. The residual coefficient ε is set as 0.01. In that case, for any $k \leq 4$, $a_i > 0$ holds for any $i \in [1, k]$. The optimal aggregate power consumption can be easily obtained based on Algorithm 1 for the continuous transmit powers. For the scenarios of discrete transmit powers, we denote the experimental results obtained from the approximation algorithm, i.e., Algorithm 3, as RMDLPSI-k SIC.

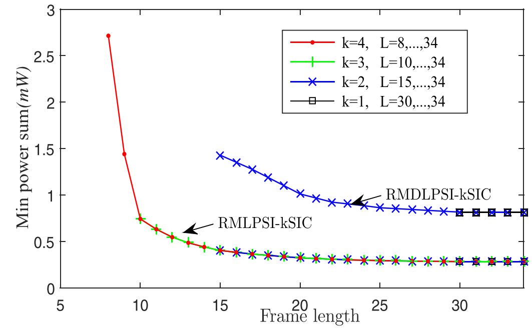

Fig. 3. Aggregate power consumption with frame length bound.

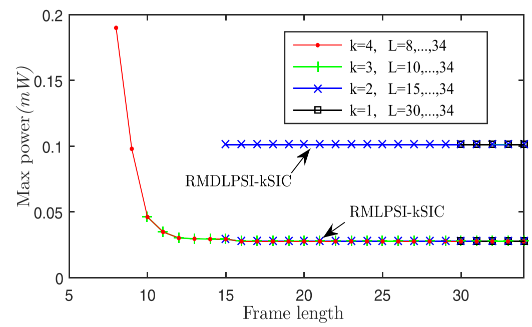

Fig. 4. Maximal transmit powers with frame length bound.

Obviously, if the given frame length L is smaller, the aggregate power consumption will be larger. In our experiments, the frame length is set from $\lceil 30/k \rceil$ to 34, i.e., the real-time performance requirement varies from the tightest to the loosest. All experimental results in this section are similar to those in [1], where perfect SIC is assumed.

The experimental results are illustrated in Fig. 3, where for equal frame lengths, the aggregate power consumption is not affected by k. The result is consistent with Lemma 4.

The case where $n = kL$ holds is termed as FSC (full slot case) for convenience. Starting from FSC, the aggregate power consumption decreases exponentially with the increasing frame length bound. From Fig. 3, we find that the aggregate power consumption is 2.7 mW when $k = 4$ and $L = 8$, while it is 1.45 mW when $k = 4$ and $L = 9$. In other words, the power saving is prominent near the FSCs. However, it will diminish exponentially if the frame length bound continues growing. Similar results can also be found for Algorithm 3.

With different values of k and L, the maximum transmit powers among the 30 UEs are illustrated in Fig. 4, which is similar with Fig. 3. Obviously, for all FSCs, the smaller the k, the less the maximum transmit power. Besides, similar to the aggregate power consumption, if the frame length bounds are same, the maximum transmit powers are also the same and are independent of k if $n \leq kL$. Furthermore, it also decreases exponentially if the real-time performance requirements are slightly relaxed

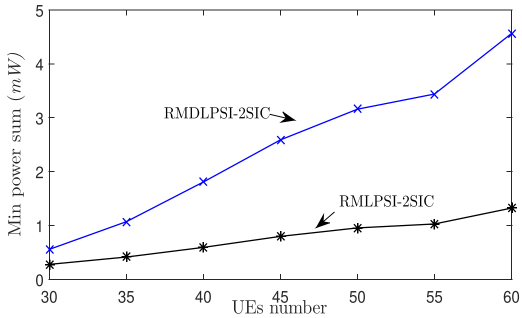

Fig. 5. Aggregate power consumption with number of UEs.

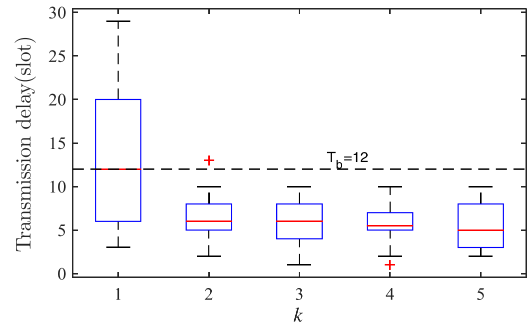

Fig. 6. Real-time performance with k.

from the FSC. Take for example $k = 4$ and $L = 8$, the maximum transmit power is 0.19 mW, while for the case of $k = 4$ and $L = 9$, it is 0.1 mW. The maximum transmit power will decrease exponentially if the frame length bound grows. All of the results are consistent with Lemma 4.

From Fig. 4, we find that in all cases where $k \leq 2$, with discrete transmit powers, the maximum transmit powers are always larger than those with continuous transmit powers,[17] and their ratios are basically the same. The reason is as follows. On one hand, for RMLPSI-k SIC, all maximum transmit powers in the considered cases with $k \leq 2$ are nearly the same, which is consistent with Lemma 4. On the other hand, the power adjusting operation in the third line of Algorithm 3 equalizes the discrete transmit powers further. We can expect that the maximum discrete transmit power will be larger for larger ρ.

The results of the above experiments revealed that, when compared to the number of parallel transmitters supported by the SIC receiver, the frame length bound has a tremendous impact on both the aggregate power consumption and the maximum transmit power. Besides, starting from the FSCs, both the aggregate power consumption and the maximum transmit power will exponentially decrease with the degradation of the real-time performance requirement.

For typical values of k, we note that the maximum transmit power is acceptable. For example, if the value of k is three, the maximum transmit power is only 0.045 mW, and it is 0.03 mW when $k = 2$, for the cases of discrete transmit powers, which are completely acceptable nowadays even for low-power RF chips. In other words, with the optimal power scheduling strategy, SIC technology is even suitable for low-power UEs even it is imperfect.

Using the default parameter settings and $L = 30$, we illustrate the relationship between the aggregate power consumption and the UE number in Fig. 5. In both cases, the aggregate power consumptions increase linearly with UE number. In other words, the average power consumption is not influenced by the UE number. Besides, the increasing rate is larger in the discrete power case, which is obviously due to the discreteness of transmit power.

[17]Since the decoding threshold is $\rho\gamma$ in Algorithm 3, for all experiments with $k > 2$, k-PTSI does not exist. Thus, the experiment with $k > 2$ is not necessary.

B. Real-Time Performance

Using the time span of a slot as the basic time unit, we assume that the sampling cycles of all UEs are the same, and the sampling cycle is denoted by T_s. The maximal delay bound is denoted by T_b, which is the real-time performance bound, and the number of UEs is n.

Obviously, only if $2L \leq T_b \leq T_s$ holds, real-time performance will be guaranteed. Therefore, $\lfloor T_b/2 \rfloor$ is the maximal value for L to guarantee the delay performance. Based on Lemma 4, if k is no less than $\lceil n/L \rceil$, every UE will be given a transmit opportunity in a frame. Therefore, for any packet of any UE, the delay time is no more than T_b, i.e., real-time performance is guaranteed.

The above method may result in so large a value of k that it is not acceptable in practice. However, the value of k could be smaller if we know the specific number of transmitters, which is denoted by $\hat{n}$, at the beginning of each frame. In that case, if $k \geq \lceil \hat{n}/L \rceil$, the real-time performance can still be satisfied.

The next experiment is to verify the real-time performance using the default network parameters. Other parameter settings specific to the experiment are as follows: $T_b = 12$, $T_s = 18$, $L = 6$, and the sampling times of the 30 UEs start uniformly in [0,17]. In view of the above analysis, if $k \geq 3$, no transmission delay[18] will be larger than T_b in high probability. Otherwise, real-time performance will not be guaranteed, although most of the transmission delays are less than T_b. The statistics of the transmission delays of all UEs are shown in Fig. 6,[19] where the x-axis is k and the y-axis is the transmission delay.

From Fig. 6, we can observe that, almost half of the packets have delays larger than T_b when $k = 1$, only one packet has delay larger than T_b when $k = 2$, and all packet delays are less than T_b when $k \geq 3$. Obviously, they are consistent with our expectations, since a smaller k means less throughput, which results in extra buffering delays of data packets.

We have some discussions on the impact of the number of UEs, i.e., n, on the delay performance. Actually, it is closely related with k, T_s, and T_b. In the worst case, i.e., $T_s = T_b$, only if

[18]The transmission delay of a packet is the time span from the generation of the packet to its being received by the sink.

[19]The experimental results have nothing to do with the adopted power scheduling algorithm because algorithms in this paper are used to generate an eligible power scheduling strategy with the minimum aggregate power consumption instead of delay.

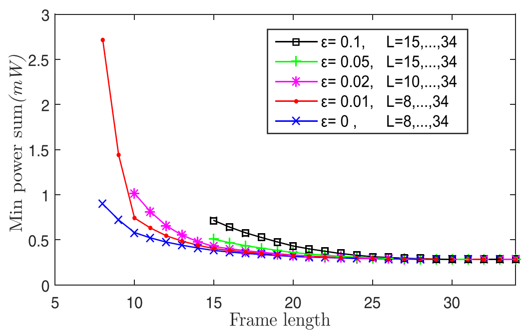

Fig. 7. Aggregate power consumption with residual coefficient.

TABLE II
APPROXIMATION RATIO OF ALGORITHM 3

L	Approximation ratio	Upper bound
15	2.46	8
20	2.19	8
25	2.02	8
28	2	8
29	1.98	8
30	1.95	4
31	1.95	4

$n \le k\lfloor T_b/2 \rfloor$, the delay performance can be guaranteed. If $T_s > T_b$, n can be larger because fewer UEs simultaneously request transmission. Take the case of this experiment for example, if the sampling times start uniformly in $[0, T_s - 1]$ and $n \le kT_s$, the delay performance can also be guaranteed. The conclusion is verified in Fig. 6.

C. Power Consumption With Residual Coefficient

We will reveal how the aggregate power consumption is influenced by the residual coefficient in this section. The decoding threshold γ is set as two and the value for k is two. Further, the residual coefficient ε is set as 0, 0.01, 0.02, 0.05, and 0.1, respectively, such that the sufficient and necessary condition in Theorem 1, i.e., $\varepsilon\delta^k < 1$, is satisfied for every ε.

The results are illustrated in Fig. 7. Obviously, the larger the residual coefficient, the larger is the aggregate power consumption, which coincides with the intuition since larger power will be paid to overcome larger residual error. Besides, with the increasing delay bound, the residual coefficient has a decreasing influence on aggregate power consumption. Since there are less parallel UEs with increasing delay bound, the influence of residual coefficient will gradually diminish.

D. Approximation Ratio

For RMDLPSI-k SIC, to compute the approximation ratio, we have to find the optimal solution. To speed up, we find it using a heuristic algorithm. The heuristic algorithm is in fact a stochastic descent algorithm as follows. Starting from the UE scheduling strategy output by Algorithm 3, we first compute the optimal power consumption of the given strategy, which is the sum of the minimum power consumption in every time slot. The minimum power consumption in any time slot can be known by a simple brute-force search. Second, we randomly choose two UEs and exchange their positions in the scheduling strategy, and then, compute the minimum power consumption of the newly generated scheduling strategy. If it is lower, the newly generated UE scheduling strategy is accepted, otherwise, it is discarded. The process continues iteratively until the aggregate power consumption is convergent.

The approximation ratios for some typical cases are listed in Table II. We also list the approximation ratio upper bound given by Theorem 4.2. Obviously, the actual approximation ratios are far below the upper bound values in all cases.

TABLE III
PERFORMANCE COMPARISON USING ALGORITHM 1 AND CPLEX (UNIT: ms)

$\gamma = 1.5$

L \ ε	0		0.01		0.05		0.1	
15	20.63	(224)	20.53	(243)	20.87	(248)	20.23	(236)
20	23.07	(230)	22.52	(218)	21.47	(245)	26.47	(224)
30	21.30	(221)	22.30	(243)	21.20	(258)	21.00	(230)

$\gamma = 2.5$

L \ ε	0		0.01		0.05		0.1	
15	21.20	(218)	21.57	(248)	22.67	(230)	21.47	(245)
20	23.20	(239)	26.30	(220)	25.30	(242)	26.35	(262)
30	22.37	(236)	22.50	(245)	23.40	(281)	21.73	(253)

E. Algorithm Complexity

In general, it has high time complexity to solve RMLPSI-k SIC with the conventional optimization-based methods, because formulation (1) is a MINP problem. By presenting the structural characteristics of the optimal solution, just as those revealed by Theorem 1 and Lemma 4, solving can be accelerated. So, the complexity of our algorithm must be greatly simplified than those based on general optimization algorithms. In order to show the advantage of our algorithm, we take RMLPSI-k SIC as an example, and compare the execution time of Algorithm 1 and the general optimization-based algorithm.

Since formulation (1) is a MINP instead of a convex problem, solving the problem using a popular optimization tool like CPLEX is experimentally proved unfeasible. Therefore, for having a feasible comparison, we first run Algorithm 1 and find the optimal UE scheduling strategy. Then, given the optimal UE scheduling strategy, the RMLPSI-k SIC, which is now a linear programming problem, can be found by CPLEX. In the last step, we compare its execution time with that of Algorithm 1. Although the comparison is unfair for Algorithm 1, the experimental results still show that Algorithm 1 takes far less time than the optimization-based algorithms. The time performance for some typical cases is listed in Table III. For every experimental case parameterized by the combination of frame length and residual coefficient, the execution times using Algorithm 1 and

CPLEX are listed, where the value in the bracket is for CPLEX. According to the result, the execution time of Algorithm 1 is around 20 ms, and that of CPLEX is around 230 ms when the optimal UE scheduling strategy is given. So, we can conclude that the time for the traditional searching algorithm to solve RMLPSI-k SIC is much longer than that of Algorithm 1.

VIII. Conclusion

This paper focuses on the tradeoff between power consumptions and real-time performance requirements of uplink transmissions for imperfect SIC-based wireless networks. We solve this problem by developing optimal power scheduling algorithms. Our conclusions are as follows: 1) under a given sufficient and necessary condition, the problem is solvable in $O(n^2)$ time in the case of continuous transmit powers, and an optimal power scheduling strategy is obtained in this paper; 2) the requirement of real-time performance has a major impact on power consumption than other factors, such as the number of simultaneous transmitters supported by imperfect SIC receiver; and 3) under the same given condition, the problem in the case of discrete transmit powers can be solved by an approximation algorithm with time complexity of $O(n^2)$.

Although the power-domain NOMA is proposed for improving spectral efficiency, it is also suitable for delay-bounded applications in IWNs. By fine-grained power scheduling, low-power consumption performance under given delay guarantee can still be provided, which makes power-domain NOMA an ideal choice for IWNs.

Appendix

A. Proof of Lemma 2

Proof. Since $\left(\widehat{X}_r^{(r)}, \widehat{X}_{r-1}^{(r)}, \ldots, \widehat{X}_1^{(r)}\right)$ is r-PTSI. $\widehat{X}_j^{(r)} = \gamma(\sum_{i=1}^{j-1} \widehat{X}_i^{(r)} + \varepsilon \sum_{i=j+1}^{r} \widehat{X}_i^{(r)} + n_0)$. Therefore, $\widehat{X}_{j+1}^{(r)} = \frac{\gamma+1}{\gamma\varepsilon+1} \widehat{X}_j^{(r)}$, i.e., r-PTSI is a geometric sequence.

In (2c), by substituting $\widehat{X}_i^{(r)}$ with $\left(\frac{\gamma+1}{\gamma\varepsilon+1}\right)^{i-1} \widehat{X}_1^{(r)}$, $\widehat{X}_1^{(r)} = \frac{\gamma n_0}{\delta_{r-1} - \gamma \sum_{i=0}^{r-2} \delta^i}$, where $\delta = \frac{\gamma+1}{\gamma\varepsilon+1}$ and $r \geq 2$. So, $\widehat{X}_i^{(r)} > 0$ holds for $\forall i \in [1, r]$, if and only if $\frac{\gamma n_0}{\delta^{r-1} - \gamma \sum_{i=0}^{r-2} \delta^i} > 0$, or equivalently $\varepsilon\delta^r < 1$. In all, r-PTSI exists if and only if $\varepsilon\delta^r < 1$. ■

B. Proof of Lemma 3

Proof. 1) With the Gaussian elimination, the matrix A can be transformed into the upper triangular matrix B using an elementary row transformation matrix $T_{r\times r}$. Besides, since all diagonal elements of A are 1 while all of the lower off-diagonal elements of A are negative, $T_{r\times r}$ is thus non-negative, which can be directly obtained from Gaussian elimination.

Furthermore, because $T_{r\times r}$ is a non-negative elementary row transformation matrix, and all elements of A in the upper diagonal are negative, $b_{ij} \leq 0$ holds for all b_{ij} in B.

2) Sufficiency. If $\varepsilon\delta^r < 1$, r-PTSI exists. For convenience, r-PTSI is denoted by $\widehat{X}^{(r)}$. Since $A\widehat{X}^{(r)} = N$ and $T_{r\times r}$ is an non-negative elementary row transformation matrix, $B\widehat{X}^{(r)} = TN > 0$. Further, since $\widehat{X}^{(r)} > 0$ and $b_{ij} \leq 0$ for all b_{ij} in B, $a_i > 0$ holds for all $i \in [1, r-1]$.

Necessity. If $a_i > 0$ for all $i \in [1, r-1]$, we can find a unique positive solution to equalities $BX = TN$ as follows.

Denote $TN = (c_1, c_2, \ldots, c_r)^T$. The unique solution $X = (X_r, X_{r-1}, \ldots, X_1)^T$ to the equalities $BX = TN$ is obviously $\left(\frac{c_r}{a_{r-1}}, \frac{c_{r-1} - X_r b_{(r-1)r}}{a_{r-2}}, \ldots, c_1 + \sum_{i=r}^{2} \gamma X_i\right)^T$. Since $X > 0$ and $AX = N$, $\varepsilon\delta^r < 1$ holds based on Lemma 2.

3) Because $T_{r\times r}$ is a non-negative elementary row transformation matrix, any vector $\overline{X}$ satisfying $A\overline{X} \geq N$ also satisfies $B\overline{X} \geq TN$. Besides, any vector $\overline{X}$ satisfying $A\overline{X} = N$ also satisfies $B\overline{X} = TN$.

Since $\widehat{X}^{(r)}$ satisfies the equations $B\widehat{X}^{(r)} = TN$, $B\big(\overline{X} - \widehat{X}^{(r)}\big) \geq 0$ for any vector $\overline{X}$ satisfying $A\overline{X} \geq N$. The last element of the vector $B\big(\overline{X} - \widehat{X}^{(r)}\big)$ is $a_{r-1}\left(\overline{X}_r - \widehat{X}_r^{(r)}\right)$, $\overline{X}_r \geq \widehat{X}_r^{(r)}$ thus holds because $a_{r-1} > 0$ and $B\big(\overline{X} - \widehat{X}^{(r)}\big) \geq 0$. Similarly, $\overline{X}_{r-1} \geq \widehat{X}_{r-1}^{(r)}$ also holds because $a_{r-1} > 0$, $a_{r-2} > 0$, $b_{(r-1)r} \leq 0$, and $B(\overline{X} - \widehat{X}^{(r)}) \geq 0$. Iteratively, since $a_i > 0$ for any $i \in [1, r-2]$, all $b_{ij} \leq 0$ for any $i \in [2, r-2]$ and $j \in [3, r]$, $\overline{X}_i \geq \widehat{X}_i^{(r)}$ for any $i \in [1, r-2]$. Therefore, $\overline{X} \geq \widehat{X}^{(r)}$.

4) Assume $\exists i \in [1, r-1]$ such that $a_i \leq 0$. Using a similar proof as 3, $p_i < 0$ must be true to ensure the existence of solutions to $AX \geq N$, which leads to contradictions. ■

C. Proof of Theorem 1

Proof. 1) Sufficiency. If $\varepsilon\delta^r < 1$, based on Lemma 3, $\sum_{i=1}^{r} \overline{X}_i \geq \sum_{i=1}^{r} \widehat{X}_i^{(r)}$ holds for any feasible solution $\left(\overline{X}_r, \overline{X}_{r-1}, \ldots, \overline{X}_1\right)$ to MPAr PT. Therefore, $\sum_{i=1}^{r} \frac{\widehat{X}_i^{(r)}}{G'_i} \leq \sum_{i=1}^{r} \frac{\overline{X}_i}{G'_i}$, where $\{G'_1, G'_2, \ldots, G'_r\}$ is any permutation of $\{G_1, G_2, \ldots, G_r\}$.

Since $\widehat{X}_r^{(r)} \geq \widehat{X}_{r-1}^{(r)} \geq \cdots \geq \widehat{X}_1^{(r)}$ and $G_r \geq G_{r-1} \geq \cdots \geq G_1$, based on the ordering inequality theorem, we know that $\sum_{i=1}^{r} \frac{\widehat{X}_i^{(r)}}{G_i} \leq \sum_{i=1}^{r} \frac{\widehat{X}_i^{(r)}}{G'_i}$.

Combining the above two inequalities together, we get $\sum_{i=1}^{r} \frac{\widehat{X}_i^{(r)}}{G_i} \leq \sum_{i=1}^{r} \frac{\overline{X}_i}{G'_i}$. Since $\left(\frac{\widehat{X}_r^{(r)}}{G_r}, \frac{\widehat{X}_{r-1}^{(r)}}{G_{r-1}}, \ldots, \frac{\widehat{X}_1^{(r)}}{G_1}\right)$ is a feasible solution to MPAr PT, and $\{\frac{\overline{X}_r}{G'_r}, \frac{\overline{X}_{r-1}}{G'_{r-1}}, \ldots, \frac{\overline{X}_1}{G'_1}\}$ represents any feasible solution to MPAr PT, $\left(\frac{\widehat{X}_r^{(r)}}{G_r}, \frac{\widehat{X}_{r-1}^{(r)}}{G_{r-1}}, \ldots, \frac{\widehat{X}_1^{(r)}}{G_1}\right)$ is thus the optimal solution to MPAr PT.

Necessity. If $\left(\frac{\widehat{X}_r^{(r)}}{G_r}, \frac{\widehat{X}_{r-1}^{(r)}}{G_{r-1}}, \ldots, \frac{\widehat{X}_1^{(r)}}{G_1}\right)$ is the optimal solution to MPAr PT, $A\widehat{X}^{(r)} \geq N$ holds, and $B\widehat{X}^{(r)} \geq TN > 0$.

We now prove the necessity by contradiction. Assume there is an $l \in [1, r-1]$ which satisfies $a_l \leq 0$, and $a_h \geq 0$ for all $h \in [l+1, r-1]$. Since for all b_{ij} in B, $b_{ij} \leq 0$ holds based on Lemma 3.1. On the other hand, to satisfy $B\widehat{X}^{(r)} > 0$, $\widehat{X}_h^{(r)} > 0$ for any $h \in [l+1, r]$ and $\widehat{X}_l^{(r)} < 0$ must hold simultaneously, which contradicts with the prerequisite $\widehat{X}^{(r)} > 0$.

2) It follows from Lemma 3.2 and Lemma 3.4. ■

D. Proof of Lemma 4

Proof. Based on the pigeonhole principle, for the optimal power scheduling strategy, assume there is a slot S_1 which has less than $\lfloor n/L \rfloor$ parallel UEs; there must exist another slot S_2

satisfying $|S_2| \geq 2 + |S_1|$, where $|S_1|$ is the cardinality of S_1. If the user which is decoded first in S_2 is moved to S_1, a new power scheduling strategy will thus come into being. Based on Theorem 1, since $\widehat{X}_i^{(r)} < \widehat{X}_{i+1}^{(r)}$ for any $i \in [1, r-1]$, the aggregate power consumption of the new-formed scheduling strategy is less than that of the optimal one, which contradicts the optimality.

Similarly, there could not be a slot which includes more than $\lceil n/L \rceil$ UEs. Therefore, Lemma 4.1 is proved.

To prove Lemma 4.2, assume there are q slots each of which has $\lfloor n/L \rfloor$ users. Since $q\lfloor n/L \rfloor + (L-q)\lceil n/L \rceil = n$, $q = L\lceil n/L \rceil - n$ holds. ■

E. Proof of Theorem 2

Proof. Sufficiency. 1) Based on the construction of $GH(n,k,L)$, and the mapping scheme that the edge (u_i, T_{hj}) means that u_i will be scheduled in slot h, any feasible UE scheduling strategy satisfying Lemma 4 can be mapped to a maximal matching of $GH(n,k,L)$, and vice versa. In other words, feasible UE scheduling strategies and the maximal matchings of $GH(n,k,L)$ have a one-to-one mapping.

2) For the edge (u_i, T_{hj}) in $GH(n,k,L)$, based on Theorem 1, $\frac{\widehat{x}_j}{G_i}$ is the minimal transmit power allocated to u_i if its decoding phase is j. Based on the above conclusions, for any maximal matching of $GH(n,k,L)$, its weighted sum is $nM - A$, where A is the minimum aggregate power consumption of all UEs for the corresponding scheduling strategy. So, the MWM of $GH(n,k,L)$ is the optimal solution to RMLPSI-k SIC, which is just the function of the tenth line in Algorithm 1.

Necessity. For any feasible scheduling strategy of the RMLPSI-k SIC problem, there must be a slot where there are at least $\lceil n/L \rceil$ UEs. For this slot, based on Theorem 1.2, there is no feasible power allocation strategy if $\varepsilon\delta^{\lceil n/L \rceil} \geq 1$. ■

F. Proof of Theorem 3

Proof. Let $A = \{\widehat{X}_1^{(\lfloor n/L \rfloor)}, \widehat{X}_2^{(\lfloor n/L \rfloor)}, \ldots, \widehat{X}_{\lfloor n/L \rfloor}^{(\lfloor n/L \rfloor)}\}$ and $B = \{\widehat{X}_1^{(\lceil n/L \rceil)}, \widehat{X}_2^{(\lceil n/L \rceil)}, \ldots, \widehat{X}_{\lceil n/L \rceil}^{(\lceil n/L \rceil)}\}$. We construct a sequence which includes all elements of A for $L\lceil n/L \rceil - n$ times, and all elements of B for $L - L\lceil n/L \rceil + n$ times. Then, the sequence is sorted in ascending order. For convenience, denote the sorted sequence as $\langle c_1, c_2, \ldots, c_n \rangle$, and let $\langle b_1, b_2, \ldots, b_n \rangle = \langle \frac{1}{G_n}, \frac{1}{G_{n-1}}, \ldots, \frac{1}{G_1} \rangle$. Then, the output of Algorithm 2 is the optimal solution to the following problem:

$$
\begin{aligned}
&\min_{\{X_{ij}\}} \sum_{i,j=[1,n]} X_{ij} c_i b_j \\
&\text{s.t.} \quad X_{ij} \in \{0,1\} \\
&\qquad \sum_{i=[1,n]} X_{ij} = 1 \quad \forall j \in [1,n] \\
&\qquad \sum_{j=[1,n]} X_{ij} = 1 \quad \forall i \in [1,n].
\end{aligned} \tag{5}
$$

Based on the ordering inequality theorem, the optimal solution to (5) is $\{X_{ij}\}$ where $X_{ij} = \begin{cases} 1 & \text{if} \quad i = j \\ 0 & \text{if} \quad i \neq j \end{cases}$. Since the output of Algorithm 2 is constructed to be consistent with the optimal value of $\{X_{ij}\}$, Algorithm 2 outputs an MWM of $GH(n,k,L)$.

G. Proof of Theorem 4

Proof. 1) WLOG, assume $u_1, u_2, \ldots, u_r$, where $r \leq k$, are scheduled simultaneously in one slot. Therefore, for

$$
\begin{aligned}
&\forall l \in [2, r-1], \frac{G_l[tp_l^{(\rho\gamma)}]}{\sum_{i=1}^{l-1} G_i[tp_i^{(\rho\gamma)}] + \varepsilon \sum_{i=l+1}^{r} G_i[tp_i^{(\rho\gamma)}] + n_0} \\
&\geq \frac{G_l[tp_l^{(\rho\gamma)}]}{\rho(\sum_{i=1}^{l-1} G_i tp_i^{(\rho\gamma)} + \varepsilon \sum_{i=l+1}^{r} G_i tp_i^{(\rho\gamma)} + n_0)} \geq \frac{\rho\gamma}{\rho} \\
&= \gamma, \frac{G_1[tp_1^{(\rho\gamma)}]}{\sum_{i=2}^{r} G_i[tp_i^{(\rho\gamma)}] + n_0} \geq \frac{G_l[tp_l^{(\rho\gamma)}]}{\rho(\sum_{i=2}^{r} G_l tp_i^{(\rho\gamma)} + n_0)} \geq \gamma,
\end{aligned}
$$

and $\frac{G_r[tp_r^{(\rho\gamma)}]}{\varepsilon \sum_{i=1}^{r-1} G_i[tp_i^{(\rho\gamma)}] + n_0} \geq \frac{G_r[tp_r^{(\rho\gamma)}]}{\rho(\varepsilon \sum_{i=1}^{r-1} G_i tp_i^{(\rho\gamma)} + n_0)} \geq \gamma$ because $tp_i^{(\rho\gamma)} \leq [tp_i^{(\rho\gamma)}] \leq \rho tp_i^{(\rho\gamma)}$ for $\forall i \in [1,r]$. Therefore, $([tp_1^{(\rho\gamma)}], [tp_2^{(\rho\gamma)}], \ldots, [tp_r^{(\rho\gamma)}])$ is a feasible solution to RMDLPSI-k SIC in the slot. Since the same proof is valid for other slots, Algorithm 3 outputs a feasible solution to RMDLPSI-k SIC.

2) WLOG, we still assume that $u_1, u_2, \ldots, u_r$, where $r \leq k$, are scheduled simultaneously in one slot. Since $tp_i^{(\rho\gamma)} \leq [tp_i^{(\rho\gamma)}] \leq \rho tp_i^{(\rho\gamma)}$ for $\forall i \in [1,r], \sum_{i=1}^{r} [tp_i^{(\rho\gamma)}] \leq \rho \sum_{i=1}^{r} tp_i^{(\rho\gamma)}$.

Denoting the optimal solution to RMDLPSI-k SIC in the slot as $(\widehat{tp}_1^{(\gamma)}, \widehat{tp}_2^{(\gamma)}, \ldots, \widehat{tp}_r^{(\gamma)})$ and that to RMLPSI-k SIC as $(tp_1^{(\gamma)}, tp_2^{(\gamma)}, \ldots, tp_r^{(\gamma)})$, $\sum_{i=1}^{r} \widehat{tp}_i^{(\gamma)} \geq \sum_{i=1}^{r} tp_i^{(\gamma)}$ holds since $\widehat{tp}_i^{(\gamma)} \geq tp_i^{(r)}$ for $\forall i \in [1,r]$.

For $tp_i^{(\gamma)}$, $\forall i \in [1,r]$, if we allocate power $\rho^i tp_i^{(\gamma)}$ to u_i, $(\rho tp_1^{(\gamma)}, \rho^2 tp_2^{(\gamma)}, \ldots, \rho^r tp_r^{(\gamma)})$ is a feasible solution to RMLPSI-k SIC with the decoding threshold being $\rho\gamma$. Therefore

$$
\sum_{i=1}^{r} tp_i^{(\rho\gamma)} \leq \sum_{i=1}^{r} \rho^i tp_i^{(\gamma)} \leq \rho^r \sum_{i=1}^{r} tp_i^{(\gamma)}. \tag{6}
$$

Since (6) is always satisfied for any value of r where $r \leq \lceil n/L \rceil$, $\frac{\sum_{i=1}^{n} tp_i^{(\rho\gamma)}}{\sum_{i=1}^{n} tp_i^{(\gamma)}} \leq \rho^{\lceil n/L \rceil}$. Therefore, $\frac{\sum_{i=1}^{n} [tp_i^{(\rho\gamma)}]}{\sum_{i=1}^{n} \widehat{tp}_i^{(\gamma)}} \leq \rho^{(\lceil n/L \rceil + 1)}$.

■

REFERENCES

[1] C. Xu, K. Ma, Y. Xu, Y. Xu, and Y. Fang, "Optimal power scheduling for uplink transmissions in SIC-based industrial wireless networks with guaranteed real-time performance," *IEEE Trans. Veh. Technol.*, vol. 67, no. 4, pp. 3216–3228, Apr. 2018.

[2] C. Xu, H. Ding, and Y. Xu, "Low-complexity uplink scheduling algorithms with power control in successive interference cancellation based wireless mud-logging systems," *Wireless Netw.*, vol. 25, no. 1, pp. 321–334, Jan. 2019.

[3] M. Li, X. Guan, C. Hua, C. Chen, and L. Lyu, "Predictive pre-allocation for low-latency uplink access in industrial wireless networks," in *Proc. IEEE INFOCOM Conf. Comput. Commun.*, Honolulu, HI, USA, Apr. 2018, pp. 1–9.

[4] Z. Ding, X. Lei, G. K. Karagiannidis, R. Schober, J. Yuan, and V. K. Bhargava, "A survey on non-orthogonal multiple access for 5G networks: Research challenges and future trends," *IEEE J. Sel. Areas Commun.*, vol. 35, no. 10, pp. 2181–2195, Oct. 2017.
[5] P. Swami, V. Bhatia, S. Vuppala, and T. Ratnarajah, "On user offloading in NOMA-HetNet using repulsive point process," *IEEE System J.*, vol. 13, no. 2, pp. 1409–1420, Jun. 2019.
[6] Z. Yang, Z. Ding, P. Fan, and N. Al-Dhahir, "A general power allocation scheme to guarantee quality of service in downlink and uplink NOMA systems," *IEEE Trans. Wireless Commun.*, vol. 15, no. 11, pp. 7244–7257, Nov. 2016.
[7] L. Lei, D. Yuan, C. K. Ho, and S. Sun, "Power and channel allocation for non-orthogonal multiple access in 5G systems: Tractability and computation," *IEEE Trans. Wireless Commun.*, vol. 15, no. 12, pp. 8580–8594, Dec. 2016.
[8] S. Han, X. Xu, X. Tao, and P. Zhang, "Joint power and sub-channel allocation for secure transmission in NOMA-based mMTC networks," *IEEE Syst. J.*, to be published, doi: 10.1109/JSYST.2018.2890039.
[9] Y. Liu, Z. Qin, M. Elkashlan, Z. Ding, A. Nallanathan, and L. Hanzo, "Nonorthogonal multiple access for 5G and beyond," *Proc. IEEE*, vol. 105, no. 12, pp. 2347–2381, Dec. 2017.
[10] E. Paolini, G. Liva, and M. Chiani, "Coded slotted ALOHA: A graph-based method for uncoordinated multiple access," *IEEE Trans. Inf. Theory*, vol. 61, no. 12, pp. 6815–6832, Dec. 2015.
[11] B. Wang, L. Dai, Y. Zhang, T. Mir, and J. Li, "Dynamic compressive sensing-based multi-user detection for uplink grant-free NOMA," *IEEE Commun. Lett.*, vol. 20, no. 11, pp. 2320–2323, Nov. 2016.
[12] L. P. Qian, Y. Wu, H. Zhou, and X. Shen, "Joint uplink base station association and power control for small-cell networks with non-orthogonal multiple access," *IEEE Trans. Wireless Commun.*, vol. 16, no. 9, pp. 5567–5582, Sep. 2017.
[13] H. Zhang, F. Fang, J. Cheng, K. Long, W. Wang, and V. C. M. Leung, "Energy-efficient resource allocation in NOMA heterogeneous networks," *IEEE Wireless Commun.*, vol. 25, no. 2, pp. 48–53, Apr. 2018.
[14] N. Zhang, J. Wang, G. Kang, and Y. Liu, "Uplink nonorthogonal multiple access in 5G systems," *IEEE Commun. Lett.*, vol. 20, no. 3, pp. 458–461, Mar. 2016.
[15] J. G. Andrews and T. H. Meng, "Optimum power control for successive interference cancellation with imperfect channel estimation," *IEEE Trans. Wireless Commun.*, vol. 2, no. 2, pp. 375–383, Mar. 2003.
[16] D. Tweed and T. Le-Ngoc, "Dynamic resource allocation for uplink MIMO NOMA VWN with imperfect SIC," in *Proc. IEEE Int. Conf. Commun.*, Kansas City, MO, USA, Dec. 2018, pp. 1–6.
[17] D. Tweed, S. Parsaeefard, M. Derakhshani, and T. Le-Ngoc, "Dynamic resource allocation for MC-NOMA VWNs with imperfect SIC," in *Proc. IEEE 28th Annu. Int. Symp. Perso., Indoor, Mobile Radio Commun.*, Montreal, QC, Canada, Oct. 2017, pp. 1–5.
[18] A. Celik, F. S. Al-Qahtani, R. M. Radaydeh, and M. Alouini, "Cluster formation and joint power-bandwidth allocation for imperfect NOMA in DL-HetNets," in *Proc. IEEE Global Commun. Conf.*, Singapore, Dec. 2017, pp. 1–6.
[19] B. Wang, L. Dai, Y. Yuan, and Z. Wang, "Compressive sensing based multi-user detection for uplink grant-free non-orthogonal multiple access," in *Proc. IEEE Veh. Technol. Conf.*, Boston, MA, USA, Sep. 2015, pp. 1–5.
[20] N. Bambos, S. C. Chen, and G. J. Pottie, "Channel access algorithms with active link protection for wireless communication networks with power control," *IEEE/ACM Trans. Netw.*, vol. 8, no. 5, pp. 583–597, Oct. 2000.
[21] R. J. Trudeau, *Introduction to Graph Theory*. New York, NY, USA: Dover, 2013.

Chaonong Xu received the B.S. and M.S. degrees in computer sciences from the Hefei University of Technology, Hefei, China, in 1998 and 2001, respectively, and the Ph.D. degree in computer science from the Institute of Computing Technology, Chinese Academy of Sciences, Beijing, China, in 2007.

In 2007, he joined Tsinghua University, Beijing, China, as a Postdoctoral Researcher. He is now an Associate Professor with the China University of Petroleum, Beijing, China. His research interests include embedded system and wireless networks.

Mianze Wu received the B.S. degree from the China University of Petroleum, Beijing, China, in 2017. He is currently working toward the M.S. degree with the Department of Computer Science and Technology, China University of Petroleum.

His research interests include wireless communication and networks.

Yongjun Xu received the B.S. degree from the Xi'an University of Posts and Telecommunications, Xi'an, China, and the Ph.D. degree from the Institute of Computing Technology, Chinese Academy of Sciences, Beijing, China, in 2001 and 2006, respectively.

He is now a Professor at the Institute of Computing Technology, Chinese Academy of Sciences. His research interests cover low power system and wireless sensor networks.

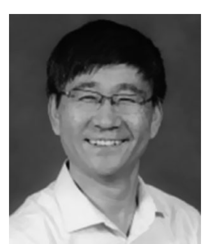

Yuguang Fang (F' 08) received the M.S. degree from Qufu Normal University, Shandong, China, in 1987, the Ph.D. degree from Case Western Reserve University, Cleveland, OH, USA, in 1994, and the Ph.D. degree from Boston University, Boston, MA, USA, in 1997.

In 2000, he joined the Department of Electrical and Computer Engineering, University of Florida, Gainesville, FL, USA, and has been a Full Professor since 2005.

Prof. Fang was the Editor-in-Chief of the IEEE TRANSACTIONS ON VEHICULAR TECHNOLOGY from 2013–2017 and IEEE WIRELESS COMMUNICATIONS from 2009–2012. He is a Fellow of the American Association for the Advancement of Science.